Hayworth KJ, Kasthuri N, Schalek R, Lichtman JW (2006) Automating the collection of ultrathin sections for large volume TEM reconstructions. Microsc Microanal 12(Suppl S02):86–87

Li A, Gong H, Zhang B, Wang Q, Yan C, Wu J, Liu Q, Zeng S, Luo Q (2010) Micro-optical sectioning tomography to obtain a high-resolution atlas of the mouse brain. Science 330:1404–1408. See the commentary by Mayerich et al

Mayerich D, Abbott LC, McCormick BH (2008) Knife-edge scanning microscopy for imaging and reconstruction of three-dimensional anatomical structures of the mouse brain. J Microsc 231:134–143

Micheva K, Smith SJ (2007) Array tomography: A new tool for imaging the molecular architecture and ultrastructure of neural circuits. Neuron 55:25–36

Ragan T, Kadiri LR, Venkataraju KU, Bahlmann K, Sutin J, Taranda J, Arganda-Carreras I, Kim Y, Seung HS, Osten P (2012) Serial two-photon tomography for automated *ex vivo* mouse brain imaging. Nat Methods 9:255–258

Tsai PS, Friedman B, Ifarraguerri AI, Thompson BD, Lev-Ram V, Schaffer CB, Xiong Q, Tsien RY, Squier JA, Kleinfeld D (2003) All-optical histology using ultrashort laser pulses. Neuron 39:27–41

White JG, Southgate E, Thomson JN, Brenner S (1986) The structure of the nervous system of the nematode Caenorhabditis elegans. Philos Trans R Soc Lond B 314:1–340

Wilt BA, Burns LD, Ho ETW, Ghosh KK, Mukamel EA, Schnitzer MJ (2009) Advances in light microscopy for neuroscience. Ann Rev Neurosci 32:435–506

Physiology and Computational Principles of Muscle Force Generation

George A. Tsianos and Gerald E. Loeb
Department of Biomedical Engineering, University of Southern California, Los Angeles, CA, USA

Definition

Muscle force generation refers to the process in which skeletal muscle, in response to neural stimuli, converts metabolic energy into active force that pulls on the bones through intermediate connective tissue.

Detailed Description

Introduction

The control problems that must be solved by the sensorimotor nervous system are determined by the complex mechanical properties of the musculoskeletal system and the even more complex and nonlinear physiological properties of muscles. Various commercial software products have been available to model musculoskeletal mechanics, but realistic models of muscle physiology are still under development. Both force generation and energy expenditure depend on both the commands from the nervous system and the kinematics of muscle length and velocity. Computational models of these processes provide the substrate upon which computational models of sensorimotor control must operate to demonstrate their feasibility.

Computational models are always approximations and usually simplifications of reality. It is usually both necessary and desirable to leave out known complexities if they do not significantly impact the particular behavior to which the model will be applied. The model presented here includes the most accurate representations currently available for the force-generating processes of individual motor units. Most previous and current research has used models that are considerably simpler, sometimes with clear justification but often from lack of consideration of relevant processes, parameters, and effects. The computational model presented here is embedded in freeware for modeling complete, arbitrary musculoskeletal systems, including their mechanical dynamics, muscles and proprioceptors, and interactions with external objects (MSMS – MusculoSkeletal Modeling Software – available from http://mddf.usc.edu). The construction of a particular model configuration and specification of its parameters, however, must come from the researcher after due consideration of the purposes of the model.

Relevant Physiology

Each muscle is controlled by a group of motoneurons known as a motor pool or motor nucleus. All motoneurons in such a pool generally receive the

same drive signals, although there are some exceptions (Loeb and Richmond 1989). Each motoneuron along with all of its muscle fibers is defined as a motor unit, whose recruitment and firing rate in response to the same drive varies substantially depending on the size and impedance of the motoneuron (Henneman and Mendell 1981). The force generated by a given motor unit at a given rate of firing depends on the total cross-sectional area of the muscle fibers in the unit.

The force production and corresponding energy consumption of each motor unit depend mainly on its length, velocity, and firing rate. Because muscle fibers within a motor unit generally have the same contractile properties, they can be lumped into one mathematical entity whose force generating capacity is proportional to the total cross-sectional area of its fibers and whose energy consumption is proportional to their volume. All of the muscle fibers in all of the motor units of a given muscle tend to move together, experiencing the same sarcomere lengths and velocities. Because of this homogeneity, most of the experimental phenomena related to contraction of whole muscle can be explained by processes occurring at the sarcomere level.

The sarcomere is the basic unit of the contractile apparatus. It is demarcated at its ends by thin Z-plates from which a matrix of thin filaments of actin projects in each direction. These interdigitate with a matrix of thick filaments of myosin that are held in the center of the sarcomere by strands of the highly elastic connectin filaments that tether the thick filaments to the Z-plates. In order for muscles to contract, protrusions from myosin called myosin heads must first be cocked to a relatively high-strain configuration and then attached to neighboring binding sites on the actin. The resulting crossbridges act like springs that pull on the actin. The metabolic energy required to cock the myosin head is provided directly by ATP molecules that are present in the sarcoplasm. In order for myosin heads to attach to neighboring binding sites, a regulatory protein called tropomyosin that normally occludes actin binding sites must undergo a conformational change. This occurs indirectly through binding of calcium to troponin, a relatively smaller molecule that is bound to tropomyosin at regular intervals along its length. When calcium binds to troponin, a local conformational change is induced that exposes nearby actin binding sites so that the cocked myosin heads can attach to form crossbridges.

The normally relaxed state of inactive muscle is achieved by ATP-powered pumping of the calcium out of the sarcoplasm and into a network of vesicles called longitudinal tubules, preventing crossbridge formation. When the muscle is activated, calcium is released from cisterns in these longitudinal tubules in response to action potentials elicited in the muscle fibers as a result of a chemical synapse with the motor axons. These action potentials propagate along the cell membrane and its invaginations deep into the muscle fiber called transverse tubules. The ATP molecules that cock the myosin heads and drive the ion pumps must be replenished eventually via catabolism of glucose occurring both in the sarcoplasm (glycolytic) and within mitochondria (oxidative), consuming additional energy. The model of muscle presented here attempts to represent each of these structures and processes as explicit terms in the set of equations that comprise the model. A model of the energetics based on these processes can be found in Tsianos et al. (2012) and is embedded in MSMS (see above).

Structure of the Model

The model is an assembly of sub-models, each characterizing a major physiological process underlying muscle contraction (Fig. 1). Modeling physiological processes independently as opposed to the aggregate behavior avoids overfitting data to specific preparations and therefore improves the likelihood that the model will be valid under untested conditions. The data driving the model originate from experiments on mammalian muscle that were designed to isolate specific processes that were then quantified. These include a wide variety of preparations with various muscle fiber architectures, but the model parameters have been normalized to dimensionless variables that depend on the constant structures of the sarcomeres, which are highly similar across all mammalian skeletal muscles.

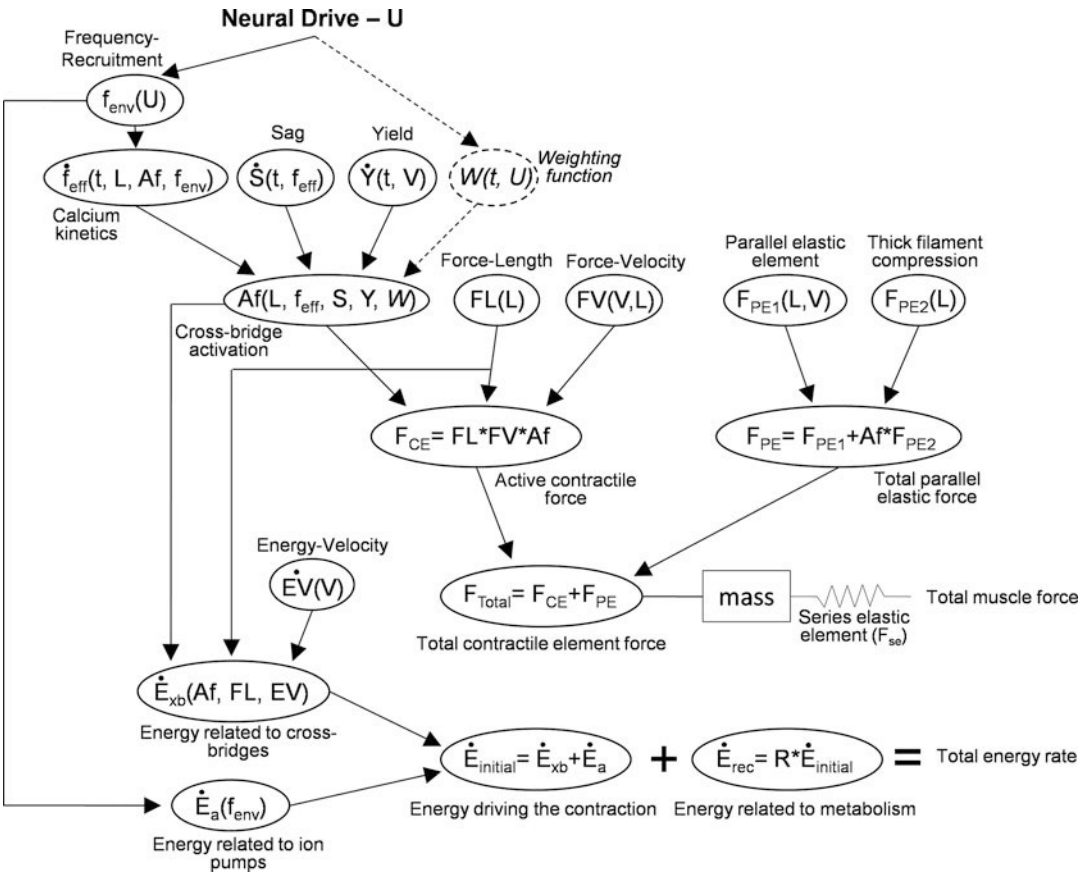

Physiology and Computational Principles of Muscle Force Generation, Fig. 1 Model overview. Independently modeled physiological processes and their contribution to muscle force production and energy consumption. (Figure from Tsianos et al. 2012, Fig. 11)

The physiological properties of muscle can change over time. In the short term, force generation may increase or decrease as a result of chemical changes associated with potentiation and fatigue, respectively. In the longer term, muscle morphology and physiology may change as a result of trophic responses to patterns of use such as exercise and injury. All of these effects tend to be specific to the various muscle fiber types, making it important to develop muscle models that reflect the subpopulations of fiber types and the relative recruitment of the motoneurons that control them. The one-to-one correspondence of the model's terms and coefficients to physiological processes makes it relatively straightforward to extend it to include unaccounted aspects of muscle contraction and to adjust its coefficients to model changes over time. Unfortunately, quantitative models of most of these time-varying processes have yet to be developed or validated.

Active Force

Frequency Recruitment As the net excitatory synaptic drive increases to a pool of motoneurons, they tend to be recruited in a fixed order from those innervating slow-twitch muscle fibers to those innervating fast-twitch muscle fibers. Increasing the drive past the threshold of a given motoneuron results in higher firing rates. This monotonic relationship can be approximated by a line whose slope depends on the recruitment threshold of the motor unit (see Fig. 2).

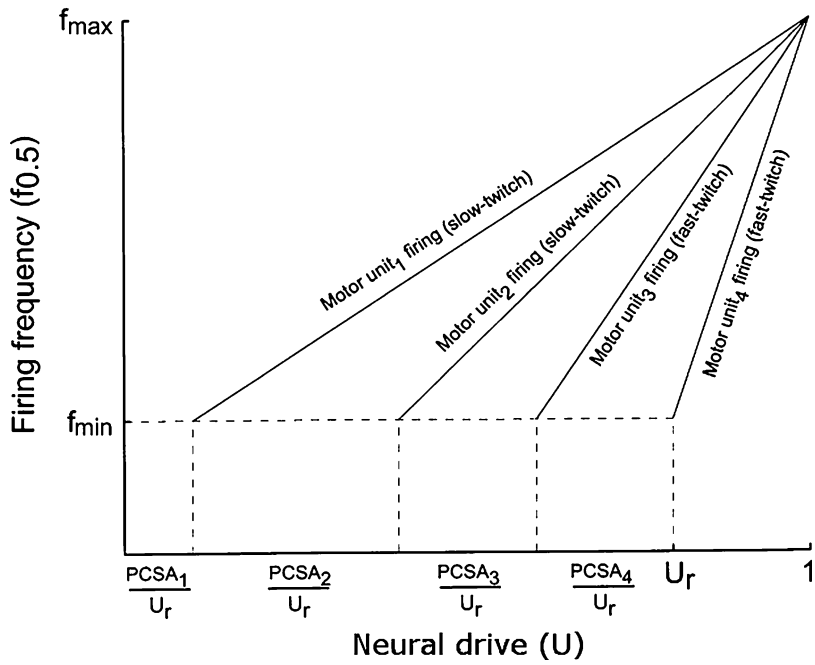

Physiology and Computational Principles of Muscle Force Generation, Fig. 2 Motor unit recruitment and modulation. The plot emphasizes the relatively higher recruitment threshold of larger motor units (e.g., *fast* vs. *slow twitch*) and their firing rate modulation until the common drive (U) saturates the firing rate of all motor units. (Figure from Cheng et al. 2000, Fig. 2)

$$f_{env_i} = f_{min} + \left(\frac{1 - U_{MU_i}^{th}}{f_{\max} - f_{\min}}\right) * U$$

Note that the firing rate is normalized to $f_{0.5}$ (frequency at which the motor unit produces half of its maximal isometric force) because motor units tend to fire between $1/2f_{0.5}$ and $2f_{0.5}$, the range over which muscle activation is most steeply modulated.

Calcium Kinetics and Crossbridge Activation (f_{eff}, Af) The sigmoidal relationship between motoneuron firing rate and activation of the contractile apparatus arises from the release, diffusion, and reuptake of calcium (see Fig. 3). At low pulse rates, the calcium released by each pulse is completely cleared before the next pulse, resulting in small, discrete twitches. As pulse rate increases, the calcium released by each pulse starts to accumulate to higher concentrations, allowing the calcium to diffuse further and expose more crossbridge binding sites. Eventually, the calcium concentration in all parts of the muscle fiber becomes sufficient to expose all binding sites and activation plateaus even if firing rate continues to increase. This is called a tetanic contraction.

The equation below captures the effects of firing rate on crossbridge activation. Y corresponds to yielding behavior exhibited by slow-twitch fibers and Sag observed in fast-twitch fibers. Both phenomena affect crossbridge activation through hypothesized mechanisms discussed in the corresponding sections. Note that equation parameter n_f is length dependent. The shape of the sigmoid relationship is defined by a_f, n_{f0}, and n_{f1} constants, some of which are fiber-type dependent. For a complete definition of all model parameters, see Tsianos et al. (2012).

$$Af(f_{\text{eff}}, L_{ce}, V_{ce}) = 1 - \exp\left[-\left(\frac{YSf_{\text{eff}}}{a_f n_f}\right)^{n_f}\right] n_f$$
$$= n_{f0} + n_{f1}\left(\frac{1}{L_{ce}} - 1\right)$$

Sag (S) When fast-twitch muscle is excited isometrically with a constant drive, its force output increases initially to some maximal level and then decreases gradually (Fig. 4). This is thought to occur due to an increase in the rate of calcium reuptake, which effectively reduces the concentration of calcium in the sarcoplasm and hence the number of crossbridges that can form.

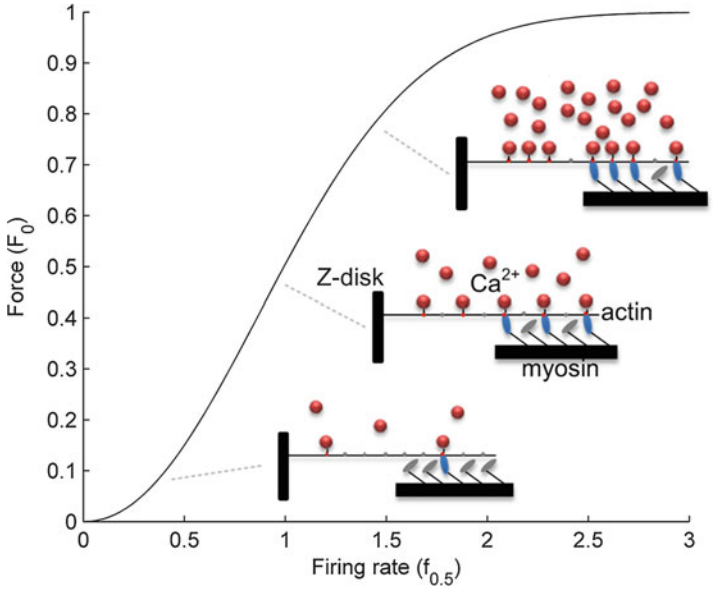

Physiology and Computational Principles of Muscle Force Generation, Fig. 3 Calcium kinetics and crossbridge activation. The effects of firing rate on isometric force output of muscle are shown from zero to tetanic activation. Overlaid graphics highlight underlying processes at the sarcomere level that give rise to the behavior. Only a small portion of the sarcomere is shown here due to symmetry. *Thick horizontal bars* represent thick filaments and *thin horizontal lines* represent thin filaments. *Vertical bars* correspond to Z-disks. The *small red spheres* are calcium ions whose bond with actin sites is indicated by *short black lines* that link them and a *small red dot* overlaid on top of the actin (*gray dots* indicate inactive binding sites). If a crossbridge is formed, then the small ovals in the figure representing myosin heads are colored *blue* and are in a cocked configuration (large angle with respect to their neck region). (Figure from Tsianos and Loeb, Muscle Physiology and Modeling, article in Scholarpedia, Fig. 3)

P

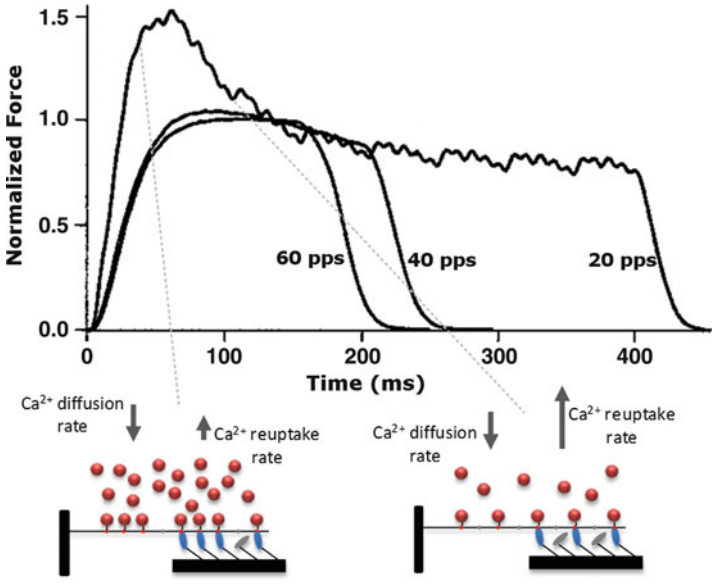

Physiology and Computational Principles of Muscle Force Generation, Fig. 4 Sag. Experimental data depicting the Sag phenomenon in response to constant stimulation for several frequencies. The graphics on the *bottom* portion illustrate the effect of increasing the rate of calcium reuptake on calcium concentration and crossbridge formation (*Top* plot from Brown and Loeb 2000, Fig. 3a. *Bottom* schematic from Tsianos and Loeb, Muscle Physiology and Modeling, article in Scholarpedia, Fig. 4)

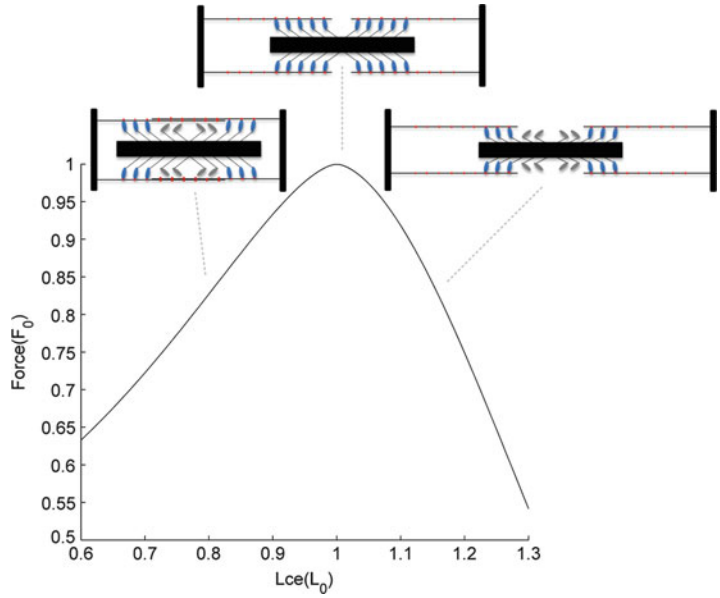

Physiology and Computational Principles of Muscle Force Generation, Fig. 5 Force-length relationship. Muscle force dependence on length is shown for tetanically stimulated muscle with minimal motion of its myofilaments. Overlaid graphics depict myofilament overlap and effects on crossbridge formation for different lengths. Note that the FL relationship does not include the steeper decline at the shortest sarcomere lengths that arises from a different mechanism. (Figure from Tsianos and Loeb, Muscle Physiology and Modeling, article in Scholarpedia, Fig. 5)

This phenomenon can be modeled by a time-varying scaling factor applied to f_{eff}, which is directly related to the calcium present in the sarcoplasm (Brown and Loeb 2000).

$$S(t, f_{\text{eff}}) = \frac{a_s - S(t)}{T_s}$$

Force-Length (FL) The amount of active force a muscle produces during maximal isometric contractions (i.e., muscle length held constant during the contraction) depends on the length at which it is fixed (Fig. 5). It produces large forces at intermediate lengths and relatively smaller forces at either shorter or longer lengths (Scott et al. 1996).

At some intermediate length, typically referred to as optimal length, overlap between thin filaments and myosin heads is maximal. Therefore, the number of crossbridges that could form and the contractile force are also maximal. Myofilament overlap is less at longer lengths, so the number of potential crossbridges and force is also smaller. Muscle force decreases at incrementally longer lengths until the point at which no more crossbridges can form and muscle can no longer produce active force. At relatively shorter lengths, thin filaments start to slide past each other (i.e., double overlap), which is thought to sterically hinder the formation of crossbridges, thereby reducing the amount of force that can be produced.

The force-length relationship, as well as all other relationships in the model, is normalized so that it generalizes across a wide range of muscle morphometries. The force corresponding to optimal length is by definition maximal, so, clearly, normalizing all force profiles to maximal isometric force under tetanic conditions provides a useful reference point. The equation capturing the normalized relationship is shown below.

$$\text{FL}(L_{ce}) = \exp\left(-\left|\frac{{L_{ce}}^{\beta} - 1}{\omega}\right|^{\rho}\right)$$

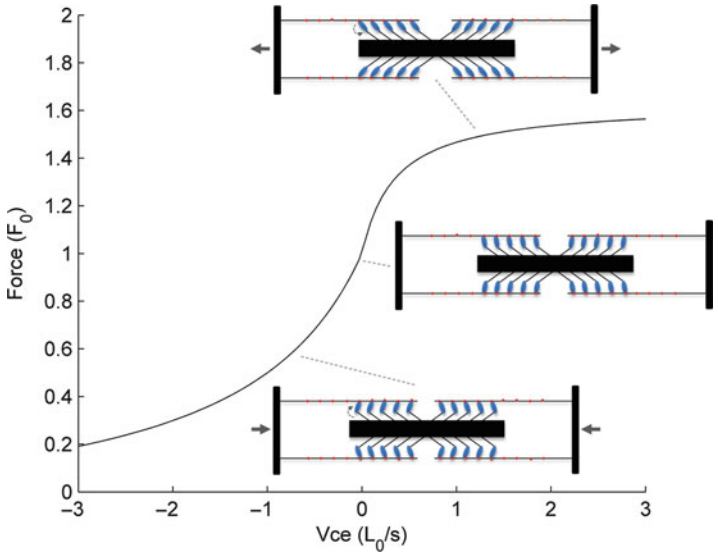

Physiology and Computational Principles of Muscle Force Generation, Fig. 6 Force-velocity relationship. Dependence on muscle force output on the velocity of stretch ($V > 0$) and shortening ($V < 0$) for tetanic stimulation at optimal muscle length. The graphics illustrate the hypothesized mechanisms for force enhancement relative to isometric in the lengthening case and depression in the shortening case. Note that in reality myosin heads do not move synchronously as shown in the figure because they are subject to thermodynamic noise and other stochastic events; the graphic illustrates their configuration on average. (Figure from Tsianos and Loeb, Muscle Physiology and Modeling, article in Scholarpedia, Fig. 6)

ω, β, and ρ are constants that define the exact shape of the inverted U and are all fiber-type dependent.

Force-Velocity (FV) Maximally stimulated muscle at a particular length produces different levels of force depending on the rate at which it is shortening or lengthening. Relative to the isometric condition, muscle produces less force while shortening and more force while lengthening (Fig. 6; Scott et al. 1996).

Shortening muscle is accompanied by motion of the attached crossbridges toward relatively less strained configurations. Larger rates of shortening increase the probability that a given crossbridge will be in a low-strain configuration; therefore, the force generated by the entire population is lower overall. By contrast, crossbridges in lengthening muscle become relatively more stretched and generate more tension until they are forcibly ripped away from the actin binding sites.

The equations below account for the discontinuous effects of the two, separate mechanisms by which velocity affects force generation:

$$\mathrm{FV}(V_{ce}, L_{ce}) = \begin{cases} (V_{\max} - V_{ce}) = V_{\max} + (c_{v0} + c_{v1} L_{ce}) V_{ce} = , V_{ce} \le 0 \\ b_v - \left(a_{v0} + a_{v1} L_{ce} + a_{v2} {L_{ce}}^2\right) V_{ce} / (b_v + V_{ce}), V_{ce} > 0 \end{cases}$$

c_{v0}, c_{v1}, and V_{max} are constants that define the shortening end of the relationship and depend on fiber type. V_{max} corresponds to the maximum velocity of shortening that the muscle fiber can undergo. The lengthening portion of the relationship is defined by fiber-type-dependent constants

b_v, a_{v0}, a_{v1}, and a_{v2}. Note that the force-velocity relationship also depends on muscle length. See "Potentiation" for a detailed description of this phenomenon as well as a mechanistic explanation.**Interactions Among Length, Velocity, and Activation**

Length Dependency of Calcium Kinetics - Changing length of the sarcomeres has effects on the calcium kinetics that govern activation. The cisterns from which the calcium is released appear to be tethered to the Z-plates at a location that is near the middle of the actin-myosin overlap when the muscle is at optimal length. At longer lengths, calcium has to diffuse over longer distances to get to the actin binding sites, which takes more time. Thus the rise times of the activation are longer (see Brown et al. 1999; Brown and Loeb 2000).

Length Dependency of Crossbridge Dynamics - Changing length of the sarcomeres has effects on the rate of attachment of crossbridges to activated and exposed binding sites on the actin. Because a muscle fiber does not gain or lose volume as it changes length, the fiber must have a larger diameter when it is at a shorter length. The hexagonally packed lattice of myofilaments in each sarcomere will then be more widely spaced, changing the distance between the myosin heads and the thin filaments where they must bind to form crossbridges. The heads are located on the ends of hinged arms containing myosin light chains, which are canted away from the longitudinal axis of the thick filament. When the sarcomere is at a long length, the myosin heads barely fit between the thick and thin filaments, so they are close to and can bind rapidly to form crossbridges. At short lengths, the myosin heads are less favorably disposed and their binding may also be affected adversely by the double overlap of the thin filaments. These effects are particularly large at lower levels of activation, where activated binding sites are more scarce on the thin filaments. The net result is shown in Fig. 7, which is based on data and models first described in Brown et al. (1999).

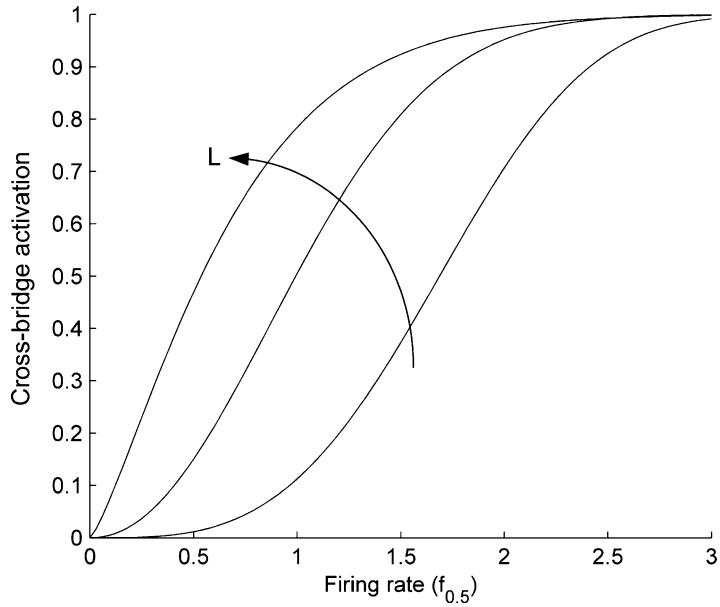

Physiology and Computational Principles of Muscle Force Generation, Fig. 7 Length dependence of crossbridge activation. Crossbridge activation is measured as the percentage of maximal force generated for a given amount of myofilament overlap (i.e., effects of myofilament overlap are removed from muscle force). Muscle length is fixed at three different values. In general, a larger portion of the available contractile machinery is activated for the same firing rate when the muscle is stretched. The *middle curve* corresponds to optimal length. (Figure from Tsianos and Loeb, Muscle Physiology and Modeling, article in Scholarpedia, Fig. 7)

The precise slope of this relationship, i.e., the sensitivity of force to firing rate, is affected by additional factors. A low firing rate activates only a small portion of the binding sites on the actin filaments. An incremental increase in the firing rate results in a relatively larger increase in the number of crossbridges formed. This is probably due to a relatively larger amount of exposed binding sites per active troponin molecule; this mechanism is known as cooperativity (Gordon et al. 2000; Loeb et al. 2002). Activation of troponin induces a local conformational change in tropomyosin, exposing neighboring binding sites on the actin. When more troponin molecules are activated along tropomyosin, a more global conformational change could be occurring, thus freeing up more actin binding sites. Crossbridge formation may also facilitate exposure of binding sites by inducing relative motion between actin and tropomyosin.

Potentiation

It was originally observed that the force generated by a single twitch of a fast-twitch muscle was much larger after a brief tetanic contraction than before. In fact, the potentiated state tends to prevail for minutes after a few, brief trains of stimulation at physiological rates, suggesting that the normal operating state of fast-twitch muscle is the potentiated state and that the conditions observed after a long period of quiescence reflect a dispotentiated state (see Brown and Loeb 1998). Furthermore, the dispotentiated state exhibits rather odd behavior such as a pronounced rightward shift in the shape of the force-length curve at subtetanic frequencies. For these reasons, the model of the fast-twitch muscle fibers presented here captures their behavior in the fully potentiated state.

Potentiation and dispotentiation phenomena appear to be related mainly to the effects of myofilament lattice spacing described above, but see also Smith et al. (2013). During dispotentiation, the light chain becomes dephosphorylated and the cant angle becomes smaller, leaving the myosin heads further from the thin filaments. The effect is greater at short lengths when the lattice spacing is large. This adversely affects the kinetics of crossbridge formation in general but more so at low firing rates when exposed binding sites are more sparsely distributed. After a few cycles of calcium release in an active muscle, the short chains become fully phosphorylated and the cant angle increases so as to position the myosin heads more favorably at short and optimal muscle lengths. At longer lengths and narrower lattice spacings, the myosin heads probably remain favorably positioned because they cannot get by the closely spaced thin filaments. The force-length relationship thus returns to the simple inverted U with maximum at optimal myofilament overlap regardless of the firing rate. Slow-twitch muscle appears to lack such a dephosphorylation process and so behaves always as if fully potentiated. The function of the dispotentiation remains obscure but may be related to minimizing "stiction," which arises when stray crossbridges in an inactive muscle form spontaneously and resist passive stretching by antagonist muscles.

The effects of sarcomere length on myofilament lattice spacing give rise to length dependencies of the force-velocity relationship that are different for slow- and fast-twitch muscle (Fig. 8). For slow-twitch muscle, the force-velocity relationship depends on length only for the lengthening condition, while fast-twitch muscle exhibits a dependency for the shortening condition. In lengthening slow-twitch muscle, smaller spacing between myosin heads and binding sites would result in a higher probability of crossbridge formation, thus leading to higher forces produced for the same velocity of stretch. This effect is also observed in dispotentiated fast-twitch muscle, but not in the potentiated state, because the reduction of interfilament spacing resulting from potentiation is thought to mask the effects of length changes (Brown and Loeb 1999). In shortening fast-twitch muscle, it is thought that smaller interfilament spacing at longer lengths increases the probability that a given crossbridge remains attached, thus making it more likely that it occupies relatively low-strain, low force configurations. Crossbridges in slow-twitch muscle stay attached for longer periods of time, which may mask the effects of length on the rate of detachment hypothesized for fast-twitch muscle.

Yield (Y) When slow-twitch muscle is submaximally stimulated at constant length and then

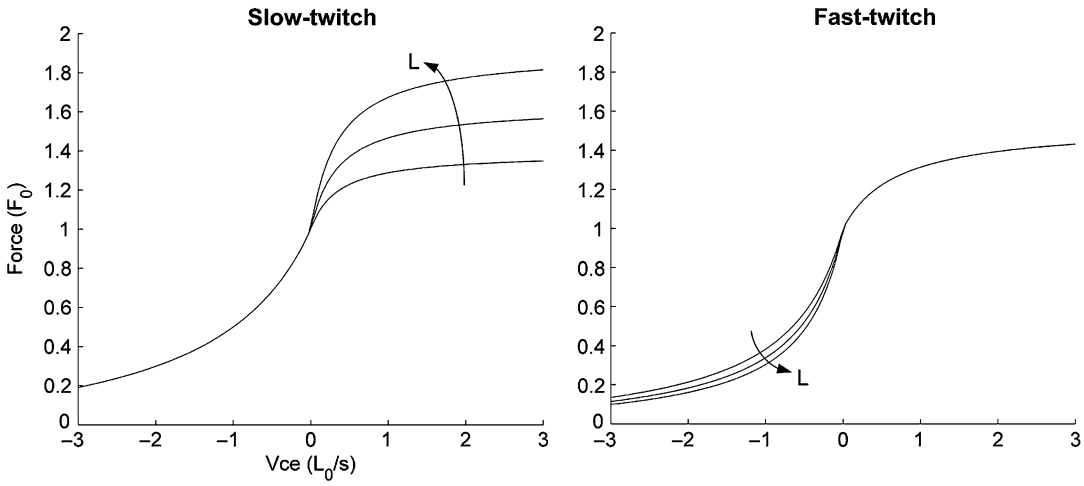

Physiology and Computational Principles of Muscle Force Generation, Fig. 8 Length dependence of force-velocity. Force-velocity curves depicting a substantial length dependency of slow-twitch muscle in the lengthening state (*left*) and fast-twitch muscle in the shortening state (*right*). See text for details. (Figure from Tsianos and Loeb, Muscle Physiology and Modeling, article in Scholarpedia, Fig. 8)

stretched *or* shortened, its force output declines (Joyce et al. 1969). This effect intensifies for lower stimulation frequencies, as shown in Fig. 9. The mechanism for this phenomenon has been hypothesized to be a reduction in the number of crossbridges attached. As muscle length changes past the stroke length of the attached crossbridges, myosin heads detach from their binding sites and must reattach to continue to produce force. The rate at which slow-twitch myosin heads can attach appears to be relatively slow compared to the rate at which binding sites slide past them, therefore making it difficult for crossbridges to reform and produce force. At lower frequencies of stimulation, relatively few binding sites are available on the helical actin, making it less likely that they will be in an appropriate orientation and distance from myosin heads for binding. By applying a time-varying scaling factor to the effective firing rate parameter, the model is able to capture this effect well (Fig. 9).

$$Y(t) = \frac{1 - c_\gamma\left[1 - \exp\left(-\frac{|V_\alpha|}{V_\gamma}\right)\right] - Y(t)}{T_y}$$

c_Y and V_Y are constants that define the intensity of the yielding effect and T_Y defines its time course.

Passive Elastic Elements

Muscle is comprised of many elastic components that generate passive forces in response to tensile or compressive strain. The aggregate force of these components may be substantial relative to the active force depending on the muscle's condition of use.

Parallel Elastic Element (F_{pe1}) Inactive muscle is under tension for about half of its anatomical range of lengths. Its passive tensile force rises exponentially over a relatively low range of lengths followed by a steep linear increase that persists all the way until maximal anatomical length (Fig. 10). The quantitative relationship for a particular muscle depends mainly on its maximal isometric force and maximal anatomical length. It is negligible over most of the range and peaks at less than 10% of F_0 at maximal anatomical length.

In frogs, this passive tension appears to arise primarily from stretching of the springlike connectin myofilaments that tether the myosin molecules to the Z-disks (Magid and Law 1985). The contribution of intermediate filaments like desmin that interconnect myofibrils within a muscle fiber has been shown to be negligible over the physiological range of sarcomere lengths (Wang

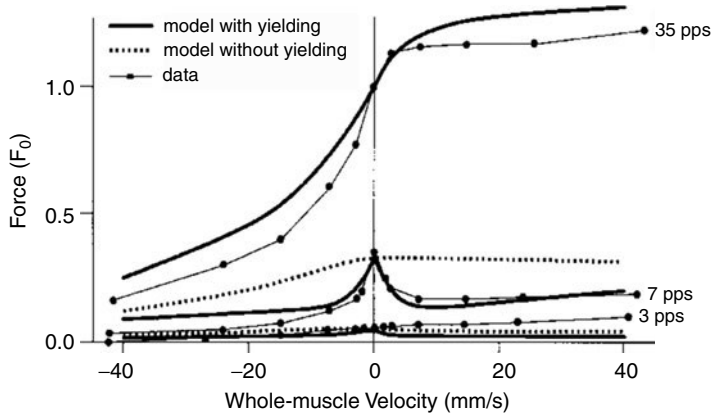

Physiology and Computational Principles of Muscle Force Generation, Fig. 9 Yielding. Plot of force-velocity relationships of slow-twitch muscle for various frequencies of stimulation. As opposed to tetanic stimulation, the force-velocity relationships for submaximal firing rates are marked by a sharper decline in force in both shortening and lengthening states relative to isometric. Experimental data and model predictions, with and without accounting for yielding, are shown. (Figure from Brown et al. 1999, Fig. 10b)

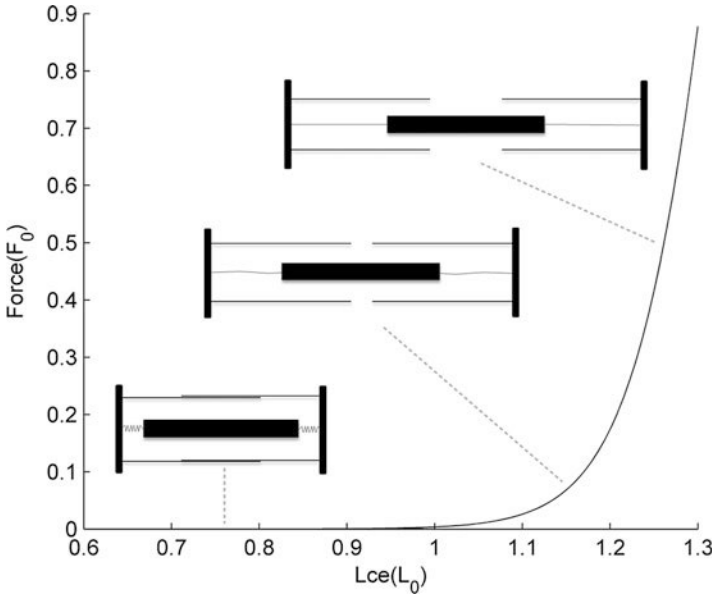

Physiology and Computational Principles of Muscle Force Generation, Fig. 10 Parallel elastic force. Passive muscle force is plotted over a representative muscle's range of motion. In general, muscles with larger anatomical ranges of motion produce less passive force at the same length (relative to optimal), that is, their passive force-length curve shifts to the right. As depicted by the superimposed schematics, some of this force results from stretching an elastic element in the sarcomere called connectin that links the thick filament to the Z-disks, but see text for the role of endomysial connective tissue. Myosin heads and actin binding sites are omitted for clarity. (Figure from Tsianos and Loeb, Muscle Physiology and Modeling, article in Scholarpedia, Fig. 10)

et al. 1993). Compared to frogs, mammalian muscles have variable but considerably more endomysial collagen surrounding each muscle fiber. This may account for substantial variation in their passive force curves, which can be substantially shifted to the left or right with respect to the

optimal sarcomere length defined by myofilament overlap (Brown et al. 1996a). This requires introduction of an additional morphometric parameter into the muscle model, L_{max}, which is based on the maximal anatomical length experienced by the muscle when attached to the skeleton. Below is the equation capturing the effect of this property on the entire passive force-length relationship.

$$F_{pe1}(L_{ce}, V_{ce}) = c_1 k_1 \ln\left\{\exp\left[\frac{L_{ce}/L_{ce}^{\max} - L_{r1}}{k_1}\right] + 1\right\} + \eta V_{ce}$$

c_1, k_1, and L_{r1} are constants defining the precise shape of the curve. Linear damping was also incorporated into the equation with constant coefficient, η, to account for the small amount of damping observed experimentally, which also contributes to the mathematical stability of the model.

Thick Filament Compression (F_{pe2}) At very short lengths, muscles generate passive force that opposes the force of contraction. This force is negligible for long lengths but starts to increase exponentially from 0.7 L_0 until the minimum physiological length where net contractile force goes to zero (see Fig. 11; Brown et al. 1996b).

The steady-state force produced by tetanically stimulated muscle decreases at a fairly constant rate for the range of lengths from L_0 to $0.7L_0$, reflecting steric interference between the overlapped thin filaments. At this relatively small length, however, the slope steepens abruptly and remains steep until the length at which net muscle force is zero. Assuming that the effects of double overlap on crossbridge formation are the same over the entire range of lengths in which it occurs, the number of crossbridges, hence force, should decrease proportionally with decreasing length. The abrupt change in force appears to reflect a collision between the myosin filament and the Z-disk, which would generate a reaction force opposing the force of contraction. The extent of compression of the myosin filament onto the Z-disk would be less for submaximal contractions because the number of crossbridges generating force would be relatively smaller. Thus it is important to model this effect separately from the force-length relationship, which affects force generation equally at all activation levels. The equation below computes the force at the muscle level as a function of length that opposes the force of contraction.

$$F_{pe2}(L_{ce}) = c_2\{\exp[k_2(L_{ce} - L_{r2})] - 1\}$$

Constants c_2, k_2, and L_{r2} define the exact shape of the relationship depicted in Fig. 11.

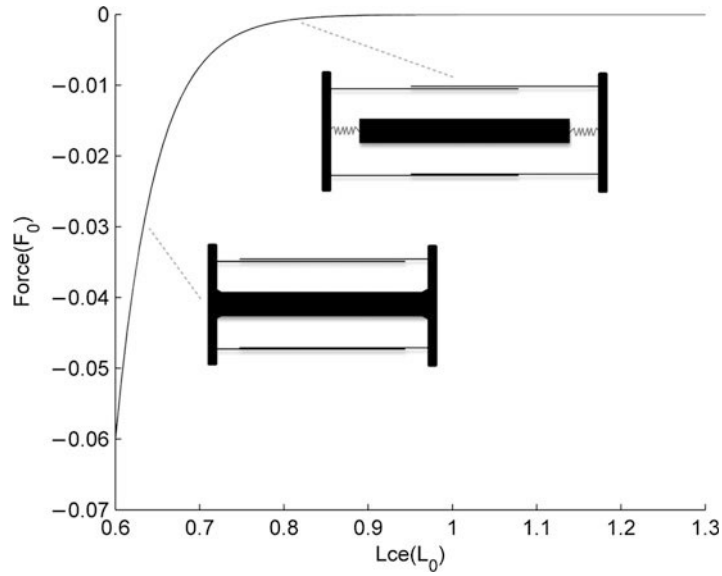

Physiology and Computational Principles of Muscle Force Generation, Fig. 11 Thick filament compression. Plot shows the parallel passive force of muscle opposing the contractile force as a function of fascicle length. The schematics illustrate the hypothesis that this force arises due to compression of the thick filament as the Z-disks are pulled even closer together at short muscle lengths. (Figure from Tsianos and Loeb, Muscle Physiology and Modeling, article in Scholarpedia, Fig. 11)

Series Elastic Element (Tendon + Aponeurosis; F_{se}) Muscles exert forces on bone segments through intermediate connective tissue, comprised mostly of aponeurosis and tendon. This serially connected tissue affects the muscle's motion, which modulates force output substantially. Clearly, the length of a muscle for a particular joint configuration depends on the length of the series elastic element because together they must span the entire path from the origin to the insertion site of the musculotendon. The portion of the path that is occupied by muscle depends not only on the resting length of the series elastic element but also on its elasticity, which determines how much it will stretch when it is pulled by the attached muscle. If a muscle is activated and then deactivated under isometric conditions as defined at the origin and insertion, the sarcomeres may experience large changes in length and especially velocity that will affect their force-generating ability. Note that the series elastic element is a nonlinear spring (see below and Fig. 12), which undergoes a substantial portion of its ultimate strain at relatively low stresses, i.e., at low levels of muscle recruitment. Under dynamic conditions of activation and kinematics, the muscle fibers may actually move out of phase with the musculotendon (Zajac et al. 1981). This has important implications for the ability of muscle spindles to encode musculotendon length, hence joint position (Hoffer et al. 1992; Scott and Loeb 1994; Mileusnic et al. 2006).

The magnitude of the effects described above depends on the ratio of the lengths of the muscle fascicles to the connective tissue in series with them. Highly pinnate muscles have short muscle fibers oriented obliquely between fascial planes called aponeuroses that merge with the external tendon. Proximally, the aponeurosis has a thin sheetlike structure with a large surface area to accommodate insertion of a large number of fibers while more distally its shape gradually becomes thicker and smaller in surface area. It has been shown experimentally that for a wide range of

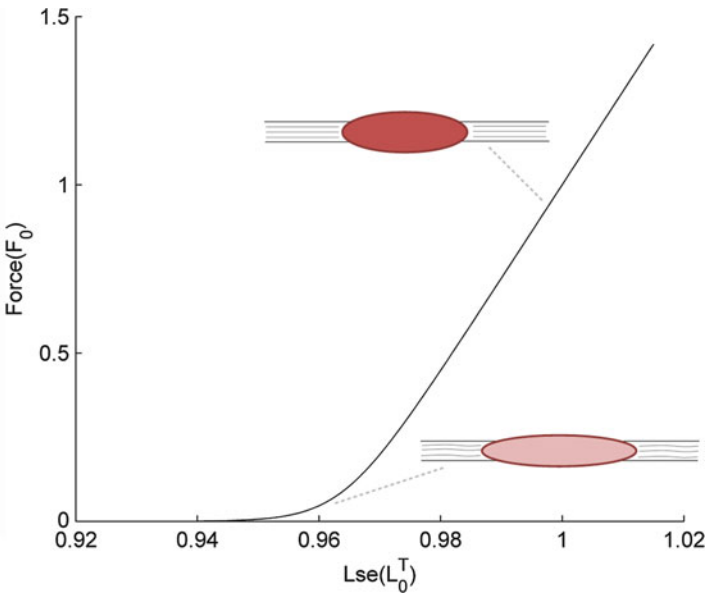

Physiology and Computational Principles of Muscle Force Generation, Fig. 12 Series elastic tendon/aponeurosis force. Force generated by elastic tissue that is in series with muscle as a function of its length. The schematic shows that for a given musculotendon length and low muscle activation (*bottom*), the tendon will be relatively slack and therefore produce little restoring force. At higher activation levels (*top*), the muscle pulls more on the tendon and causes a larger restoring force. The stiffness is also greater in this case, denoted by the increased slope of the relationship, because the tendon becomes tauter at these higher force levels. (Figure from Tsianos and Loeb, Muscle Physiology and Modeling, article in Scholarpedia, Fig. 12)

P

muscle forces, aponeurosis and tendon strain are the same (Scott and Loeb 1995). The fact that the gradual thickening of the aponeurosis is paralleled by an increase in the number of fibers that exert force on it suggests that the stresses are fairly constant along its entire length. Because the stress and strain experienced by the aponeurosis and tendon are roughly the same, then presumably their material properties are similar and they can be lumped into a single element. The absolute thickness and strength of this connective tissue element is presumably controlled by trophic factors that depend on the maximal tensile forces that it experiences. The model assumes that tendon force scales with muscle cross-sectional area, or equivalently it scales with F_0, and strain is measured with respect to tendon length at F_0 (L_0^T), permitting a generic relationship to be derived (see Fig. 12). This has been confirmed using several force-length relationships of the tendon/aponeurosis obtained experimentally (Brown et al. 1996b). L_0^T is a good normalization factor because it can be determined more reliably as opposed to the more commonly used tendon slack length. The equation that defines this relationship is shown below.

$$F_{se}(L_{se}) = c^T k^T \ln\left\{\exp\left[\frac{L_{SE} - L_r^T}{k^T}\right] + 1\right\}$$

Constants c^T, k^T, and L_r^T define the precise form of the relationship shown in Fig. 12.

Parameters Needed to Model Specific Muscles

Musculotendons are comprised of the same basic elements, such as sarcomeres for contractile elements and collagen for passive elements, whose structural organization and properties lead to substantially different behavior on the whole musculotendon level. Knowledge of musculotendon morphometry and fiber-type-specific properties of sarcomeres is crucial for tailoring the generic relationships that comprise the model to the specific muscle of interest. The general physiological models above all employ normalization to dimensionless parameters (Topp et al. 1986) and so must be converted into real physical units (e.g., cm, N) by morphometric parameters of the musculoskeletal system to be modeled.

Optimal Fascicle Length (L_0)

As mentioned in "Relevant Physiology," sarcomeres have roughly the same dimensions and experience the same range of length changes during a contraction. Longer muscle, therefore, has more sarcomeres in series. This means that a given change in muscle length of a longer muscle is accompanied by relatively smaller length changes at the sarcomere level, hence a smaller change in myofilament overlap and force produced. Because the dimensionless force-length relationship applies to behavior at the sarcomere level, it must be scaled by the length of the muscle to account for this architectural effect on the behavior of the whole muscle. The morphometric parameter used for this purpose is optimal fascicle length, which is the distance between the aponeurosis sites measured along the orientation of the muscle fibers, measured at the length for which the muscle produces its maximal isometric force. Fascicle length is measured instead of muscle belly length because muscle fibers in many muscles are oriented obliquely with respect to the long axis of the muscle belly.

Muscle Mass (m)

The amount of force that a muscle can produce depends on the total number of myofilaments arranged in parallel. Because myofilaments are densely packed through muscle fibers, this number is proportional to the physiological cross-sectional area (PCSA) of the muscle fibers. Because those fibers may be arranged in a pinnate form, the anatomical cross section of the muscle may not be perpendicular to all the muscle fibers and so would not reflect their true cross-sectional area. More reliable measurements can be made of the mass of the muscle, which can be converted to its volume by dividing by density. This volume must be the product of the length of the contractile elements (L_{ce}), which can be measured reliably by dissecting fascicles from the muscle, assuming that they are of uniform length (common) and at optimal length L_0 (any discrepancy can be

detected and corrected by observing sarcomere length under a microscope).

$$\mathrm{PCSA} = \frac{m}{\rho L_{ce}}$$

Specific tension, ε, or maximal isometric force produced per unit of cross-sectional area (Spector et al. 1980; Lucas et al. 1987), has been shown to be the same across different fiber types (31.8 N/cm^2) and can be used to estimate maximal isometric force (F_0) using the following equation:

$$F_0 = \varepsilon * \mathrm{PCSA}$$

Muscle fascicle length in the equation is set to L_0, because ε is defined at that length. The modeled muscle's F_0 is used to scale the dimensionless relationships to obtain force output in absolute units.

Fiber Composition

Although maximal isometric force per unit area is roughly the same for different muscle fiber types, there are substantial differences in their contractile properties. Fiber types differ in terms of kinematic modulation of force output, rise and fall dynamics of contraction, and especially energy consumption. The recruitment order of motor units also depends on their fiber type. It is therefore important that different fiber types are modeled independently and that the fiber composition of the modeled muscle is known accurately.

Determining fiber composition is often challenging because of the many classifications of fiber types and because of the difficulty in measuring the attributes that distinguish them. Fibers differ mainly in terms of their myosin isoforms (namely, the myosin light and heavy chains) and the size of their sarcoplasmic reticulum and transverse tubule system that together influence force generation under dynamic conditions. There are also large differences in mitochondrial content and blood supply, which affect the metabolic cost of muscle contraction as well as the fiber's susceptibility to fatigue. All of these tend to covary in healthy muscle fibers but may become heterogenous in muscle fibers that are diseased or undergoing trophic changes as a result of abnormal or rapidly changing usage patterns. Because differences in myosin heavy chain isoform and mitochondrial content have the largest physiological effects, they are used most commonly to classify fiber types. Slow-twitch (type 1) fibers have a different distribution of myosin heavy-chain isoforms than fast-twitch (type 2) fibers that leads to slower crossbridge kinetics, as evidenced by the relatively slow rate at which they hydrolyze ATP. Type 1 fibers and some type 2 fibers (namely, type 2a) have a high volume fraction of mitochondria, which can be assessed indirectly by measuring the concentrations of enzymes such as succinate dehydrogenase, for example, which is normally present in the mitochondria. These histochemical approaches require a tissue sample, which could be too invasive to obtain from humans. It is also worth noting that the results may be biased depending on the location in which it is obtained. Fast-twitch fibers tend to reside in the outer portion in muscle, so if a single sample is obtained from this location, the measurement would underestimate the percentage of slow-twitch muscle. There are also noninvasive methods for measuring fiber composition such as magnetic resonance spectroscopy, but to date they are relatively less accurate.

Characteristic Firing Rate of Muscle Fiber Type ($f_{0.5}$)

Muscles typically fire at rates ranging from $0.5f_{0.5}$ to $2f_{0.5}$, where $f_{0.5}$ is the firing rate at which muscle produces half of its maximal isometric force when its length is held at L_0. $f_{0.5}$ is an important parameter because crossbridge activation relationships of different muscles that are normalized by this value become congruent, and therefore a generic relationship can be obtained. This is useful because only this parameter is needed to construct the entire crossbridge activation relationship for an arbitrary muscle to a high degree of accuracy. The actual firing rate behavior of motor units has been difficult to record, particularly at the higher levels of recruitment, so this useful normalization remains contentious.

Tendon + Aponeurosis Length (L_0^T)

The tendon plus aponeurosis is composed of tightly packed strands of collagen that are oriented in parallel with the long axis of the musculotendon. As in muscle, the amount a tendon can stretch depends on its length and the amount of force it generates in response to a stretch depends on its cross-sectional area. Longer tendons are composed of more collagen molecules arranged in series, each having similar material properties and dimensions, i.e., experiencing the same change in length in response to the same force. Longer tendons can therefore experience larger changes in length and will produce lower forces in response to the same stretch. The generic relationship of the series elastic element reflects the material properties of the constituent collagen fibers and should be scaled by the length of the tendon plus aponeurosis to be modeled. The length should be measured when muscle is exerting maximal isometric force on the tendon (L_0^T). If only the slack length of the tendon is known, then L_0^T can be estimated as 105% of tendon slack length.

Maximum Musculotendon Path Length (L_{max}^{MT})

As mentioned in "Parallel Elastic Element," the amount of passive force generated by muscle at a particular length correlates with its maximal anatomical length. Maximal anatomical length is defined as the maximal length a muscle can have across all anatomical configurations of the joints it crosses. This can be estimated by first measuring maximal anatomical length of the musculotendon and subtracting the length corresponding to the tendon (L_0^T).

Pinnation Angle

Muscle fibers of many muscles are oriented obliquely with respect to the tendon, and so not all of the force that they generate is transmitted to the bone segments. It is reduced by the cosine of the pinnation angle, with the remainder of the contractile force producing hydrostatic compression of the muscle. Even for relatively large pinnation angles, however, this loss in total force transmission in isometric muscle is relatively low (Scott and Winter 1991), so this model does not account for this effect and does not require specification of pinnation angle. Modeling the effects of pinnation angle would be important for the relatively uncommon scenario in which it is large and changes rapidly by large amounts throughout a contraction, as it would alter the kinematics of the muscle fascicles, which in turn have a strong influence on force production.

References

Brown IE, Loeb GE (1998) Post-activation potentiation – a clue for simplifying models of muscle dynamics. Am Zool 38:743–754

Brown IE, Loeb GE (1999) Measured and modeled properties of mammalian skeletal muscle. I. The effects of post-activation potentiation on the time course and velocity dependencies of force production. J Muscle Res Cell Motil 20:443–456

Brown IE, Loeb GE (2000) Measured and modeled properties of mammalian skeletal muscle: IV. Dynamics of activation and deactivation. J Muscle Res Cell Motil 21:33–47

Brown IE, Liinamaa TL, Loeb GE (1996a) Relationships between range of motion, L0, and passive force in five strap-like muscles of the feline hind limb. J Morphol 230:69–77

Brown IE, Scott SH, Loeb GE (1996b) Mechanics of feline soleus: II. Design and validation of a mathematical model. J Muscle Res Cell Motil 17:221–233

Brown IE, Cheng EJ, Loeb GE (1999) Measured and modeled properties of mammalian skeletal muscle. II. The effects of stimulus frequency on force-length and force-velocity relationships. J Muscle Res Cell Motil 20:643

Cheng E, Brown IE, Loeb GE (2000) Virtual muscle: a computational approach to understanding the effects of muscle properties on motor control. J Neurosci Methods 101:117–130

Gordon AM, Homsher E, Regnier M (2000) Regulation of contraction in striated muscle. Physiol Rev 80: 853–924

Henneman E, Mendell LM (1981) Functional organization of the motoneuron pool and its inputs. In: Brooks VB (ed) Handbook of physiology sect I the nervous system, vol II, part 1. American Physiological Society, Washington, DC, pp 423–507

Hoffer JA, Caputi AA, Pose IE (1992) Activity of muscle proprioceptors in cat posture and locomotion: relation to EMG, tendon force and the movement of fibres and aponeurotic segments. In: IBRO symposium series, vol 1–6. Pergamon Press, Oxford

Joyce GS, Rack PMH, Westbury DR (1969) Mechanical properties of cat soleus muscle during controlled

lengthening and shortening movements. J Physiol Lond 204:461–474
Loeb GE, Richmond FJR (1989) Motor partitioning: epiphenomena masquerading as control theory. Behav Brain Sci 12:660–661
Loeb GE, Brown IE, Lan N, Davoodi R (2002) The importance of biomechanics. Adv Exp Med Biol 508: 481–487
Lucas SM, Ruff RL, Binder MD (1987) Specific tension measurements in single soleus and medial gastrocnemius muscle fibres of the cat. Exp Neurol 95: 142–154
Magid A, Law DJ (1985) Myofibrils bear most of the resting tension in frog skeletal muscle. Science 230: 1280–1282
Mileusnic MP, Brown IE, Lan N, Loeb GE (2006) Mathematical models of proprioceptors. I. Control and transduction in the muscle spindle. J Neurophysiol 96: 1772–1788
Scott SH, Loeb GE (1994) The computation of position sense from spindles in mono-and multiarticular muscles. J Neurosci 14:7529–7540
Scott SH, Loeb GE (1995) Mechanical properties of aponeurosis and tendon of the cat soleus muscle during whole-muscle isometric contractions. J Morphol 224: 73–86
Scott SH, Winter DA (1991) A comparison of three muscle pennation assumptions and their effect on isometric and isotonic force. J Biomech 24:163–167
Scott SH, Brown IE, Loeb GE (1996) Mechanics of feline soleus: I. Effect of fascicle length and velocity on force output. J Muscle Res Cell Motil 17:205–218
Smith IC, Gittings W, Huang J, McMillan EM, Quadrilatero J, Tupling AR, Vandenboom R (2013) Potentiation in mouse lumbrical muscle without myosin light chain phosphorylation: is resting calcium responsible? J Gen Physiol 141:297–308
Spector SA, Gardiner PF, Zernicke RF, Roy RR, Edgerton VR (1980) Muscle architecture and the force velocity characteristics of the cat soleus and medial gastrocnemius: implications for motor control. J Neurophysiol 44:951–960
Topp EL, Zajac FE, Stevenson PJ (1986) A dimensionless muscle-tendon model for use in computer studies of posture and movement: its static, dynamic and stiffness properties. Neuroscience 12:1424
Tsianos GA, Rustin C, Loeb GE (2012) Mammalian muscle model for predicting force and energetics during physiological behaviors. IEEE Trans Neural Syst Rehabil Eng 20:117–133
Wang K, McCarter R, Wright J, Beverly J, Ramirez-Mitchell R (1993) Visoelasticity of the sarcomere matrix of skeletal muscles. The titin-myosin composite filament is a dual-stage molecular spring. Biophys J 64: 1161–1177
Zajac FE, Zomlefer MR, Levine WS (1981) Hindlimb muscular activity, kinetics and kinematics of cats jumping to their maximum achievable heights. J Exp Biol 91:73–86

Physiology and Function of Cochlear Efferents

John J. Guinan
Eaton Peabody Laboratories, Massachusetts Eye and Ear Infirmary, Harvard Medical School, Boston, MA, USA

Synonyms

Final neurons of the descending auditory system; Medial and lateral efferents; Olivocochlear bundle; Olivocochlear efferents

Definition

Cochlear efferents are neurons that originate in the brainstem and terminate in the cochlea.

Detailed Description

Anatomy

In mammals, the final descending auditory pathways to the cochlea originate in the brainstem superior olivary complex and are called "olivocochlear efferents." They are divided into two subsystems: the medial olivocochlear (MOC) and lateral olivocochlear (LOC) efferents (Fig. 1). MOC efferents originate in the medial part of the superior olivary complex and terminate mainly on outer hair cells (OHCs). LOC efferents originate in the lateral part of the superior olivary complex and terminate mainly on the peripheral processes (dendrites) of auditory nerve fibers under inner hair cells (IHCs) (Fig. 1, bottom). Efferent fibers also have branches that innervate other structures. Both MOC and LOC neurons receive inputs from other brain areas including higher auditory centers (not shown in Fig. 1).

In many species there are approximately twice as many MOC fibers that cross the midline and innervate the contralateral cochlea compared to the MOC fibers that are uncrossed and innervate the ipsilateral cochlea. In contrast, almost